Biochimica et Biophysica Acta 1852 (2015) 1856–1866

Contents lists available at ScienceDirect

Biochimica et Biophysica Acta

journal homepage: www.elsevier.com/locate/bbadis

Epilepsy-causing mutations in Kv7.2 C-terminus affect binding and functional modulation by calmodulin

Paolo Ambrosino [a,1], Alessandro Alaimo [b,1], Silvia Bartollino [a], Laura Manocchio [a], Michela De Maria [a], Ilaria Mosca [a], Carolina Gomis-Perez [b], Araitz Alberdi [b], Giovanni Scambia [c], Gaetan Lesca [d], Alvaro Villarroel [b], Maurizio Taglialatela [a,b,e,*], Maria Virginia Soldovieri [a]

[a] Dept. of Medicine and Health Sciences, University of Molise, Campobasso, Italy
[b] Biophysics Unit, CSIC, UPV/EHU, Universidad del País Vasco, Leioa, Spain
[c] Dept. of Obstetrics and Gynecology, Catholic University of Sacred Heart, Rome, Italy
[d] Dept. of Medical Genetics, Hospices Civils de Lyon, Lyon, France
[e] Dept. of Neuroscience, University of Naples "Federico II", Naples, Italy

ARTICLE INFO

Article history:
Received 17 December 2014
Received in revised form 14 May 2015
Accepted 8 June 2015
Available online 12 June 2015

Keywords:
Calmodulin
Kv7.2
Epilepsy
Surface Plasmon Resonance
Far-Western blotting
Fluorescence
Electrophysiology

ABSTRACT

Mutations in the KCNQ2 gene, encoding for voltage-gated Kv7.2 K^+ channel subunits, are responsible for early-onset epileptic diseases with widely-diverging phenotypic presentation, ranging from Benign Familial Neonatal Seizures (BFNS) to epileptic encephalopathy. In the present study, Kv7.2 BFNS-causing mutations (W344R, L351F, L351V, Y362C, and R553Q) have been investigated for their ability to interfere with calmodulin (CaM) binding and CaM-induced channel regulation. To this aim, semi-quantitative (Far-Western blotting) and quantitative (Surface Plasmon Resonance and dansylated CaM fluorescence) biochemical assays have been performed to investigate the interaction of CaM with wild-type or mutant Kv7.2 C-terminal fragments encompassing the CaM-binding domain; in parallel, mutation-induced changes in CaM-dependent Kv7.2 or Kv7.2/Kv7.3 current regulation were investigated by patch-clamp recordings in Chinese Hamster Ovary (CHO) cells co-expressing Kv7.2 or Kv7.2/Kv7.3 channels and CaM or CaM_{1234} (a CaM isoform unable to bind Ca^{2+}). The results obtained suggest that each BFNS-causing mutation prompts specific biochemical and/or functional consequences; these range from slight alterations in CaM affinity which did not translate into functional changes (L351V), to a significant reduction in the affinity and functional modulation by CaM (L351F, Y362C or R553Q), to a complete functional loss without significant alteration in CaM affinity (W344R). CaM overexpression increased Kv7.2 and Kv7.2/Kv7.3 current levels, and partially (R553Q) or fully (L351F) restored normal channel function, providing a rationale pathogenetic mechanism for mutation-induced channel dysfunction in BFNS, and highlighting the potentiation of CaM-dependent Kv7.2 modulation as a potential therapeutic approach for Kv7.2-related epilepsies.

1. Introduction

Mutations in the KCNQ2 gene, encoding for Kv7.2 voltage-gated K^+ channel subunits, are responsible for a wide spectrum of early-onset human epileptic diseases. These range from Benign Familial Neonatal Seizures (BFNS; OMIM: 121200), an autosomal-dominant epilepsy of newborns characterized by recurrent seizures that begin in the very first days of life and remit after a few weeks or months, with mostly normal interictal electroencephalogram (EEG), neuroimaging, and psychomotor development [1,2], to epileptic encephalopathies in which pharmacoresistant seizures, distinct EEG and neuroradiological features are associated to various degrees of developmental delay (Epileptic encephalopathy, early infantile, 7; OMIM: 613720; [3,4]).

Kv7.2 subunits, in some cases together with highly homologous Kv7.3 subunits encoded by the KCNQ3 gene, underlie the M-current (I_{KM}) [5], a K^+-selective current which is suppressed by Gq-linked neurotransmitter receptors activation and plays a critical role in neuronal excitability control [6,7]. Kv7 channels are tetramers of subunits each showing six transmembrane segments (S_1–S_6), and cytoplasmic N- and C-termini of variable length. The pore domain is encompassed by the S_5–S_6 segments and the intervening linker, whereas the transmembrane segments between S_1 and S_4 form the voltage-sensing domain (VSD), with S_4 charged and uncharged residues contributing to voltage-dependent gating [8–10]. The long C-terminal domain plays a crucial role in Kv7.2 channel function and regulation: in fact, it contains

Abbreviations: Ca^{2+}, calcium; K^+, potassium; DMEM, Dulbecco's Modified Eagle's Medium; FBS, Fetal Bovine Serum; OD, optical density; CHO, Chinese Hamster Ovary; RT, room temperature; HRP, Horseradish peroxidise; IPTG, isopropyl-β-D-thiogalactoside; GST, glutathione S-transferase; CaM, calmodulin; SPR, Surface Plasmon Resonance; BFNS, Benign Familial Neonatal Seizures

* Corresponding author at: Department of Medicine and Health Sciences, University of Molise, Via De Sanctis, 86100 — Campobasso, Italy.
E-mail address: m.taglialatela@unimol.it (M. Taglialatela).

[1] P.A. and A.A. contributed equally to this work and should be considered first authors.

http://dx.doi.org/10.1016/j.bbadis.2015.06.012
0925-4439/

domains required for homomeric or heteromeric subunit assembly (sid) [11,12] and for a complex network of mutually interacting molecules, such as phosphatidylinositol 4,5-bisphosphate (PIP_2; [13]), calmodulin (CaM; [14,15]), syntaxin-1A [16], A-kinase-anchoring proteins (AKAPs), which allows Kv7 channel regulation by protein kinase C (PKC; [17]), and ankyrin-G (Ank-G; [18]). A complex interplay among these regulatory molecules is suggested by the observation that they often bind to overlapping regions within the Kv7.2 C-terminus; in fact, the CaM binding site, which involves two putatively α-helical regions (A and B helices; see Fig. 1A), partially overlaps with that for PIP_2 [19], AKAPs [20], syntaxin-1A [21] and contains putative phosphorylation sites for PKC [14,17]. The pathophysiological role of the C-terminal region in Kv7.2-related epilepsies is suggested by this region being a hot-spot for disease-causing mutations [3]; among these, we have recently described Kv7.2 mutations falling within the A (W344R, L351F, L351V) or the B (R553Q) helices, or in the A–B interhelical region (Y362C) in a large cohort of BFNS-affected families [22]; therefore, in the present work, the biochemical and functional consequences prompted by these mutations on CaM binding and CaM-dependent functional regulation were investigated. To this aim, biochemical studies were performed using both Far-Western blotting, which provides semi-quantitative information, and quantitative Surface Plasmon Resonance (SPR) and dansylated CaM fluorescence assays to investigate the interaction of CaM with a Kv7.2 C-terminal fragment encompassing the A and B helices. In parallel, possible mutation-induced changes in CaM-dependent Kv7.2 and Kv7.2/Kv7.3 current regulation were investigated by patch-clamp recordings in Chinese Hamster Ovary (CHO) cells co-expressing Kv7.2 and/or Kv7.3 subunits and CaM; furthermore, to investigate whether the observed functional changes were dependent on the Ca^{2+}-binding ability of CaM, electrophysiological experiments were also carried out using a modified CaM unable to bind Ca^{2+} (CaM_{1234}) [23,24].

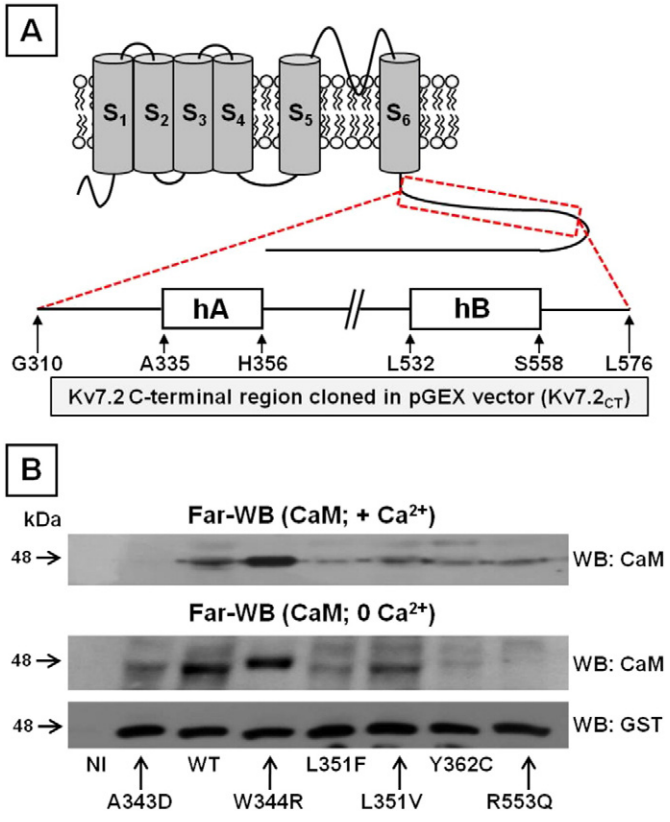

Fig. 1. Interaction between $Kv7.2_{CT}$ and CaM studied by Far-Western blotting. A) Topological representation of a Kv7.2 subunit. The red box indicates the fragment of the C-terminal domain (from G310 to the L576 residues) cloned in pGEX vectors; the "hA" and "hB" marked boxes indicate the A and B α helical regions involved in CaM binding to Kv7.2 channels [14]. B) Representative image of Far-Western blot experiments using bacterial lysates expressing wt or mutant GST-$Kv7.2_{CT}$ (prey) and GST-CaM (bait) proteins. The interaction between GST–$Kv7.2_{CT}$ and CaM was tested both in the presence (upper panel) and in the absence (middle panel) of Ca^{2+}. In the lower panel, a representative image of an anti-GST western-blot performed using the same quantities of total bacterial lysates loaded in the upper panels, to check for equal loading of IPTG-induced GST–$Kv7.2_{CT}$ fragments is reported.

2. Materials and methods

2.1. Plasmid preparation

Plasmids for bacterial (pGEX-KG) or mammalian (pcDNA3.1) CaM expression were kindly provided by Prof. M. S. Shapiro (University of Texas at San Antonio, Texas, USA); plasmids for bacterial expression of Kv7.2 C-terminal fragments encompassing the CaM binding site (GST-$Kv7.2_{CT}$; from G310 to L576, numbering according to the longest Kv7.2 isoform a, GenBank accession no. NM_172107.2) were engineered as previously described [14]. The full-length Kv7.2 plasmid (encoding for variant c, GenBank accession no. NM_004518.4) was kindly given by Dr. Thomas J. Jentsch (Department of Physiology and Pathology of Ion Transport, Leibniz-Institut für Molekulare Pharmakologie, Berlin, Germany). BFNS-associated mutations (W344R, L351F, L351V, Y362C, R553Q; [22]) were introduced in these plasmids by using Quick-change mutagenesis, as previously described [25]. The successful introduction of mutations was checked by direct sequencing of the entire coding region.

2.2. Recombinant calmodulin expression and purification

The expression of CaM and wild-type (wt) or mutant Kv7.2 C-terminal fragments was obtained adapting previously described protocols [26]. Briefly, DH5α bacterial cells were transformed with pGEX plasmids encoding for the proteins of interest fused to the glutathione S-transferase (GST) coding sequence. Individual fresh colonies corresponding to each positive clone were inoculated in 10 ml of LB and incubated for 12-16 h at 37 °C. These cultures were subsequently used to inoculate 1 l of LB medium and incubated at 37 °C until the $OD_{550\ nm}$ reached 0.5-0.6, when the cultures were added with 0.5 mM isopropyl-β-D-thiogalactoside (IPTG) and left at 37 °C for 4 h to induce the recombinant protein expression. Successful expression of each protein was checked by comparing total protein lysates from non-induced or IPTG-induced bacterial lysates on 10% polyacrylamide gels. GST-CaM purification under native conditions was then obtained by bacterial culture centrifugation at 12,000 *g* for 10′ at 4 °C, followed by pellet resuspension in GST buffer (containing 20 mM Tris–HCl, 100 mM NaCl, 1 mM EDTA, 0.5% Triton X-100, 1× protease inhibitors and lysozyme, pH 8; [14]) and sonication in ice for 6 cycles, each lasting 10 s with a 10 s interval in between. For GST-CaM purification, a chromatographic column was loaded with Glutathione Sepharose 4B (GE Healthcare, Piscataway, New Jersey, USA), washed with distilled H_2O to remove the excess of ethanol and equilibrated with GST buffer. Finally, the column was loaded with 0.22 μm-filtered soluble fraction of the bacterial suspension and left on a rotating wheel platform for 16 h at 4 °C: after a GST washing, proteins bound were eluted by adding 10 mM reduced glutathione dissolved in 50 mM Tris pH 8, and 5 fractions of 1 ml were collected. Aliquots of each fraction were run on 10% polyacrylamide gels in parallel with non-induced/IPTG-induced bacterial cultures to check for successful CaM purification in the soluble fraction and to identify the highest concentrated fraction to be used in the following experiments (Suppl. Fig. 1A).

2.3. Recombinant Kv7.2 constructs production and purification

The previously described protocol for CaM only allowed recovering of GST-$Kv7.2_{CT}$ fragments in the insoluble fraction (Suppl. Fig. 1B), irrespective of the presence of different or higher concentrations of

detergents (0.5% Igepal, 1% sarcosyl, 2% Triton) in the suspension buffer (data not shown). As protein extraction from this fraction is very inefficient, often requiring the addition of denaturing detergents, recombinant proteins from total lysates were used as previously described [27]. To quantify induced proteins in total lysates, aliquots of IPTG-induced total bacterial lysates expressing wt GST–Kv7.2$_{CT}$ fusion proteins were run on 10% polyacrylamide gels, in parallel with an aliquot of non-induced total lysate (Suppl. Fig. 1C); then, the strip of the gel containing the non-induced and the first aliquot of the IPTG-induced lysate was Blue-stained (staining solution contained 45% MetOH, 45% acetic acid, 0.01% Blue Coomassie) and used as reference to identify the uncolored part of the gel containing the protein of interest. This was excised from the gel and incubated for 16 h at 37 °C in an elution buffer, containing (in mM): 50 Tris–HCl, 150 NaCl, 0.1 EDTA; pH 7.5. The suspension was then centrifuged at 8000 rpm for 10′ at RT and the protein concentration of the supernatant was determined by using a bovine serum albumin calibration curve. Therefore, known quantities of the protein lysates were run on 10% polyacrylamide gels to check the successful GST-Kv7.2$_{CT}$ protein purification and to find the linearity range for quantification of wt and mutant GST-Kv7.2$_{CT}$ recombinant proteins in total bacterial lysates (Suppl. Fig. 1D).

2.4. Western and Far-Western blotting experiments on bacterial lysates

Western- and Far-Western blotting experiments were performed as previously described [28]. Briefly, total lysates containing 15 μg of recombinant GST–Kv7.2$_{CT}$ proteins (prey) were separated on 10% polyacrylamide gels and transferred for 1 h at 100 V at 4 °C on polyvinylidene difluoride (PVDF, Biorad, Milan, Italy) membranes. In western-blotting experiments, membranes were incubated in 5% casein dissolved in PBS-2% Tween (PBS-T) for 1 h at RT, to reduce unspecific binding, before incubation with rabbit polyclonal anti-GST antibodies (1:10.000; GE Healthcare) for 16 h at 4 °C and with anti-rabbit HRP-conjugated secondary antibodies (1:5000; GE Healthcare) for 1 h at RT. Reactive bands were detected by chemiluminescence (ECL Western blotting Susbtrate; Promega Corporation). Images were captured, stored, and analyzed with the ImageLab, version 4.1 analysis software (Bio-Rad Laboratories, Milan, Italy).

In Far-Western blotting experiments, membranes were incubated in renaturating buffer (RenB: 100 mM NaCl, 20 mM Tris–HCl pH 7.6, 0.5 mM EDTA, 10% glycerol, 0.1% Tween, 2% casein, 1 mM dithiothreitol) and reacted with gradually decreasing concentrations of guanidine hydrochloride (Applichem, Darmstadt, Germany). Then, membranes were incubated in 5% casein dissolved in PBS-T 1 h at RT before incubation for 16 h at 4 °C with 5 μg of purified CaM (bait) dissolved in RenB buffer. Unbound proteins were removed by washing with PBS-T for 30 min; membranes were then incubated with mouse monoclonal anti-CaM antibodies (1:500; Millipore, Billerica, MA, USA) for 16 h at 4 °C and anti-mouse HRP-conjugated secondary antibodies (1:5000; GE Healthcare). In Ca^{2+}-free experiments, casein was omitted and 10 mM EDTA was added to all solutions. Acquisition and data analysis was performed as above described.

2.5. Surface Plasmon Resonance (SPR) assays

Surface Plasmon Resonance (SPR) assays were performed as previously described [29]. Briefly, experiments were performed at 25 °C using a Biacore T100 instrument (GE Healthcare) and CM5 chips, provided of carboxymethyl dextran surface activated using a mixture of 0.4 M 1-ethyl-3-(3-dimethylaminopropyl)-carbodiimide (EDC) and 0.1 M N-hydroxysuccinimide (NHS) at a flow rate of 10 μl/min for 7 min using a running buffer (RB), containing (in mM): 10 HEPES pH 7.5, 150 NaCl, 4 $CaCl_2$, 0.005% P-20 surfactant (GE Healthcare). Ca^{2+} concentrations were chosen in analogy to previously reported studies [30,31]. Optimal pH for CaM (ligand) immobilization was obtained when 50 ng/μl GST-CaM was diluted in 10 mM NaAcetate pH 3.5 (the isoelectric point of the GST-CaM is 4.56 when measured with the DNASTAR/LaserGene/EditSeq software, version 7.1.0). After binding signal reached 4000 response units (RU), 1 M ethanolamine-HCl pH 8.5 was injected at a flow rate of 10 μl/min for 7 min of contact time to deactivate remaining active ester groups. A single flow cell on the chip was activated and deactivated without ligand immobilization and used as reference channel to subtract unspecific binding to the chip.

After GST-CaM immobilization, each bacterial lysate containing recombinant Kv7 fragments (analyte) diluted in RB was injected for 250 s (association time) from the lowest (0 nM; in double) to the highest (5000 nM) concentration, followed by 300 s of dissociation time. After each injection, the chip surface was regenerated by a single 20 s injection with 20 μl/min 10 mM EGTA, followed by four injections each lasting 10 s with 30 μl/min of 20 mM NaOH. Sensorgrams obtained after RB injection (blank) in parallel experiments were subtracted from binding signals to remove unspecific binding to CaM. Binding data were analyzed using the BiaEvaluation Software 2.1 (GE Healthcare) and the best fit to the experimental data was obtained by using the conformational change model, described by the following equation:

$$dAB/dt = (k_{a1} * A * B - k_{d1} * AB) - (k_{a2} * AB - k_{d2} * AB')$$

where AB and AB′ indicate the concentrations of the complex conformational states. From this equation, the dissociation constants (K_D) were measured as follows:

$$K_D = (K_{d1}/K_{a1}) * [K_{d2}/(K_{d2} + K_{a2})].$$

Non determined K_D values were obtained when binding signals were not correctly fitted to this equation.

2.6. Fluorometric measurements using dansylated-calmodulin

Recombinant proteins encoding wt or mutant (W344R, L351F, L351V, Y362C, R525Q or A343D) Kv7.2 CaM binding domain fused to GST (GST-Kv7.2$_{CT}$), were expressed in the BL21-DE3 strain of *Escherichia coli* and obtained principally as inclusion bodies. These proteins were refolded and purified following the procedures reported in the literature [32]. Recombinant CaM was also produced in BL21-DE3 cells and purified as previously described [32]. Fluorescent dansylated CaM (D-CaM, 5-(dimethylamino)naphtalene-1-sulfonyl-calmodulin) was prepared using recombinant CaM and dansyl chloride, as described [33]. Dispersion of the samples was evaluated by dynamic light scattering (DLS) using a Zetasizer Nano instrument (Malvern Instruments Ltd., Malvern, UK) in order to exclude the presence of aggregates.

Prior to the experiments, D-CaM and GST–Kv7.2$_{CT}$ constructs were dialyzed for 48 h against 2 L of fluorescence buffer containing (in mM) 25 Tris–HCl (pH 7.4), 120 KCl, 5 NaCl, 2 $MgCl_2$, 10 EGTA; the buffer was changed every 12 h. Steady-state fluorescence measurements were performed at RT with an Aminco Bowman series 2 (SLM Aminco) fluorescence spectrophotometer in a final volume of 100 μl (using quartz cuvette). The excitation wavelength was 340 nm and emissions were recorded from 400 to 660 nm. Slit widths were set at 4 nm for both excitation and emission.

Titration experiments were performed reacting increasing concentrations of GST-Kv7.2$_{CT}$ fusion proteins in fluorescence buffer with 12.5 nM D-CaM. Experiments were also performed in the presence of an excess of free Ca^{2+} (3.9 or 100 μM), adding 9.63 or 9.985 mM Ca^{2+} to the fluorescence buffer. The data obtained at lower (3.9 μM, presented in this report) and higher (100 μM) free Ca^{2+} concentrations were indistinguishable. Free Ca^{2+} concentrations were determined using Fura-2 (Invitrogen), following the manufacturer's instructions.

Fluorescence enhancement was plotted against GST-Kv7.2$_{CT}$ protein concentration and concentration–response curves were obtained by fitting a Hill equation to the data (fluorescence increase $= A \times [Ligand]^h / EC_{50} + [Ligand]^h$, where A is the maximal fluorescence increase and h is

the Hill coefficient), allowing to estimate the apparent affinity (EC_{50} or concentration that gives half-maximal change in fluorescence emission intensity) and Hill coefficient. Data are shown as average of at least four independent experiments.

2.7. Cell culture and transfections

CHO cells were grown in 100 mm plastic Petri dishes in Dulbecco's Modified Eagle Medium (DMEM) containing 10% fetal bovine serum (FBS), penicillin (100 IU/ml), and streptomycin (100 IU/ml) in a humidified atmosphere at 37 °C with 5% CO_2. For electrophysiological experiments, the cells were seeded on glass coverslips (Carolina Biological Supply Company, Burlington, NC, USA) and transfected the next day using Lipofectamine 2000 (LifeTechnologies, Milan, Italy). Plasmids encoding for Kv7.2, Kv7.3 and CaM were transfected using different cDNA ratios (ranging from 1:1 to 1:10); total cDNA in the transfection mixture was kept constant at 4 μg (for electrophysiological experiments) or at 6 μg (for biotinylation experiments).

2.8. Cell surface biotinylation and Western blotting

Plasma membrane expression of wt and mutant Kv7.2 subunits in CHO cells co-expressing CaM or CaM_{1234} (transfection ratio 1:5) was investigated by surface biotinylation of membrane proteins in transfected cells 24 h after transfection using Sulfo-NHS-LC-Biotin (Pierce), a cell-membrane impermeable reagent, as previously described [22]. Following cell transfection, biotinylation, and lysis (in a buffer containing 2% Triton, 20 mM Tris–HCl pH 7.5, 120 mM NaCl, 50 mM KCl, 10 mM EDTA, 50 mM NaF, 2 mM DTT), cell lysates were reacted with ImmunoPure immobilized streptavidin beads (Pierce). Channel subunits in streptavidin precipitates and remaining total lysates were analyzed by Western blotting on 8–12% SDS-PAGE gels using mouse monoclonal anti-Kv7.2 (clone N26A/23, dilution 1:1000; UC Davis/NIH NeuroMab Facility, Davis, CA, USA) or mouse monoclonal anti-CaM (05–173; 1:1000; Millipore, Billerica, MA, USA) antibodies, followed by HRP-conjugated anti-mouse secondary antibodies (clone NA931V; dilution 1:5000; GE Healthcare). Reactive bands were detected by chemiluminescence (ClarityTM Western ECL Substrate; Biorad). To confirm that the biotinylation reagent did not leak into the cell and label intracellular proteins and to check for equal protein loading, the same blots were also probed with anti-α-tubulin antibodies (dilution 1:5000; Sigma). Acquisition and data analysis were performed by using ImageLab software (version 4.1; Bio-Rad).

2.9. Whole-cell electrophysiology

Macroscopic currents from transiently-transfected CHO cells were recorded at RT 24 h after transfections, with an Axopatch 200A amplifier (Molecular Devices, Union City, CA, USA) using the whole-cell configuration of the patch-clamp technique and glass micropipettes of 3–5 MΩ resistance. The extracellular solution contained (mM): 138 NaCl, 5.4 KCl, 2 $CaCl_2$, 1 $MgCl_2$, 10 glucose, and 10 HEPES, pH 7.4 with NaOH. The pipette (intracellular) solution contained (mM): 140 KCl, 2 $MgCl_2$, 10 EGTA, 10 HEPES, 5 Mg-ATP, pH 7.3–7.4 with KOH. The pCLAMP software (version 10.2; Molecular Devices) was used for data acquisition and analysis.

Linear cell capacitance (*C*) was determined by integrating the area under the whole-cell capacity transient, evoked by short (5–10 ms) pulses from −80 to −75 mV with the whole-cell capacitance compensation circuit of the Axopatch 200A turned off. All illustrated and analyzed currents were corrected offline for linear capacitance and leakage currents using standard subtraction routines of the Clampfit module of pClamp10. Current densities (expressed in pA/pF) were calculated as peak K^+ currents at 0 mV divided by *C*. Data were acquired at 0.5–2 kHz and filtered at 1–5 kHz with the 4-pole low-pass Bessel filter of the amplifier. No corrections were made for liquid junction potentials.

2.10. Statistics

Data are expressed as the mean ± SEM. Statistically-significant differences between the data ($p < 0.05$) were evaluated with the Student's *t*-test or by one-way analysis of variance (ANOVA), followed by the Newman–Keul test for comparison among multiple groups.

3. Results

3.1. Interaction between $Kv7.2_{CT}$ and CaM studied by Far-Western blotting

Epilepsy-causing mutations in Kv7.2 often affect the cytoplasmic C-terminal region, an attachment site for several regulatory molecules [34,35]. To investigate whether epilepsy-causing mutations in this region of Kv7.2 channels interfere with the binding of the ubiquitous Ca^{2+}-sensing protein CaM, Far-Western blotting experiments were performed. To this aim, wt or mutant GST–Kv7.2 C-terminal fragments ($Kv7.2_{CT}$; Fig. 1A) carrying the following mutations: W344R, L351F, L351V, Y362C, or R553Q (naturally-occurring and disease-causing) [22], or the A343D (which is known to abolish CaM binding and was therefore used as negative control) [32,36] were used. IPTG-induced bacterial cell lysates containing 15 μg of each of these constructs were separated on polyacrylamide gels and, after protein renaturation, membranes were incubated with 5 μg of purified CaM, both in the presence and absence of Ca^{2+}; anti-CaM antibodies were then used in Western-blots to reveal possible mutation-induced changes in $Kv7.2_{CT}$/CaM interaction. As shown in Fig. 1B (upper panel), in the presence of Ca^{2+}, a specific 50 kDa band corresponding to the expected molecular mass of the GST–$Kv7.2_{CT}$ fusion protein was detected in all lanes except in that corresponding to A343D [32,36]. However, when compared to $wtKv7.2_{CT}$, the intensity of the W344R band was stronger ($n = 4$; $p < 0.05$ *versus* wt) or lower in the case of L351F, Y362C or R553Q ($n = 3$–4; $p < 0.05$ *versus* wt); by contrast, no changes in the intensity of L351V ($n = 3$; $p > 0.05$ *versus* wt) was detected. Upon Ca^{2+} removal (Fig. 1B, middle panel), the signals for L351F, L351V, Y362C or R553Q were significantly reduced compared to $wtKv7.2_{CT}$ ($n = 3$; $p < 0.05$ *versus* wt), whereas the W344R band was of similar intensity ($n = 3$; $p > 0.05$ *versus* wt). In this experimental condition, the band corresponding to A343D was also visible, although its intensity was much lower than that of $wtKv7.2_{CT}$ ($n = 3$; $p < 0.05$ *versus* wt). Noteworthy, the possibility that the observed changes in band intensities could be accounted for by differences in the amount of loaded proteins is ruled out by the results of Western blot experiments using anti-GST antibodies which failed to reveal any change in band intensity between wt and mutant $Kv7.2_{CT}$ (Fig. 1B, lower panel). Although Far-Western blotting experiments only provide semi-quantitative data, these results suggest that the Kv7.2 mutations herein investigated significantly and differentially alter CaM interaction, both in the presence and in the absence of Ca^{2+}.

3.2. Interaction between $Kv7.2_{CT}$ and CaM investigated by Surface Plasmon Resonance (SPR)

To examine in more detail the impact of the mutations of interest on the $Kv7.2_{CT}$/CaM interaction, Surface Plasmon Resonance (SPR) experiments, similar to those recently performed to investigate the interaction of Kv7.1 C-terminal domain with the accessory subunit KCNE1 [37], were performed. To this aim, increasing concentrations (0–1000 nM) of $Kv7.2_{CT}$ from IPTG-induced bacterial lysates (quantified as described in Suppl. Fig. 1C–D) were perfused onto CM5 chips where CaM had been previously immobilized (see *Methods* section for details); data were only obtained in the presence of Ca^{2+}, as CaM immobilization on the SPR chip was not achieved when Ca^{2+}-free solutions were used (data

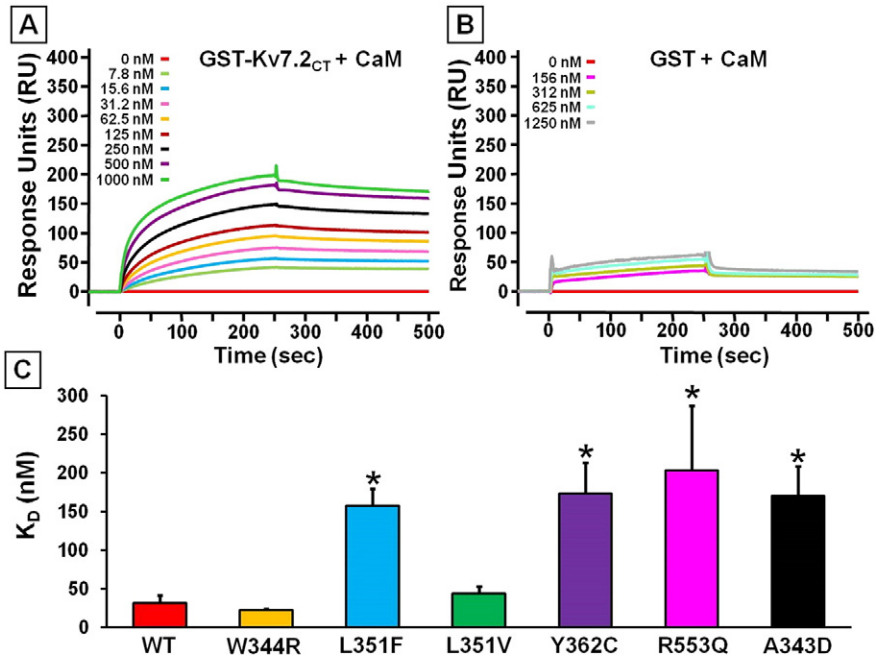

Fig. 2. Interaction between $Kv7.2_{CT}$ and CaM investigated by Surface Plasmon Resonance (SPR) assays. A–B) Representative curves showing the increase (association phase) or the decrease (dissociation phase) in the response units when native CaM, immobilized on the chip, reacted with total bacterial lysates expressing GST–$Kv7.2_{CT}$ (A) or only GST (B) proteins. Each color corresponds to binding sensorgrams obtained using different induced protein concentrations, as indicated. C) Quantification of dissociation constants (K_D) measured as described in *Methods* section. Asterisks indicate values significantly different ($p < 0.05$) versus wt$Kv7.2_{CT}$. Each bar is the mean ± SEM from 4 independent experiments.

not shown). Binding sensorgrams for CaM interaction with IPTG-induced lysates from bacteria transformed with GST–$Kv7.2_{CT}$ or with the empty vector (GST only) are shown in Figs. 2A and B, respectively. Fitting $Kv7.2_{CT}$ sensorgrams to a conformational change binding model resulted in a K_D value of 31.5 ± 10.2 nM for CaM ($n = 8$); by contrast, no binding could be detected when bacterial lysates containing 0–1250 nM GST were perfused on the same chip. Instead, a significant decrease in binding affinity was measured when fragments carrying the A343D mutation were perfused (K_D = 169.8 ± 38.3 nM; $n = 5$; $p < 0.05$ *versus* wt). Similar results were obtained with L351F, Y362C, or R553Q mutant constructs (K_D values were 157.8 ± 21.5 nM, 173.3 ± 39.6 nM, and 203.2 ± 83.9 nM, respectively; $n = 4–6$; $p < 0.05$ *versus* wt; $p > 0.05$ *versus* A343D–$Kv7.2_{CT}$). By contrast, W344R or L351V mutant constructs displayed K_D values (22.2 ± 2.0 nM and 44.0 ± 9.5 nM, respectively; $n = 4$; $p > 0.05$ *versus* wt) similar to those of wt$Kv7.2_{CT}$; noteworthy, consistent with the Far-Western blotting results (see Fig. 1B, upper panel), W344R/CaM binding affinity showed a tendency to be slightly higher (lower K_D value) than that of wt$Kv7.2_{CT}$, although the data failed to reach statistical significance.

3.3. Interaction between $Kv7.2_{CT}$ and CaM studied by dansyl-CaM fluorescence

Technical limitations precluded the assessment of the impact of the mutations in the absence of Ca^{2+} by SPR. To fill this gap, we turned to the dansyl-CaM (D-CaM) fluorescence assay; D-CaM is a CaM fluorescent derivate that reports the binding to target peptides, Ca^{2+} or both, based on the fluorescence enhancement occurring when the environment of the dansyl group becomes hydrophobic [38]; we have previously applied this technique to the study of CaM/$Kv7.2_{CT}$ interaction [31]. To this aim, D-CaM (12.5 nM) was incubated with increasing concentrations (6.25–800 nM) of GST or GST–$Kv7.2_{CT}$ (wt or mutant), both in the presence and in the absence of a physiologically relevant concentration (3.9 μM) of free Ca^{2+}, and the changes in fluorescence emission induced by their interaction were measured (Fig. 3; Table 1). GST alone had no effect on the fluorescence spectrum of D-CaM both in the presence and in the absence of Ca^{2+} (data not shown); similarly, we were unable to detect any significant interaction between D-CaM and the A343D, both in the presence and in the absence of Ca^{2+} (black plots in Figs. 3A and B, respectively) [32]. wt$Kv7.2_{CT}$ (red plots in Fig. 3) caused a saturable, concentration-dependent fluorescence enhancement, indicating a direct interaction of this protein with CaM. The introduction of mutations in helix A (W344R, L351F, L351V), in the interhelical linker (Y362C), or in the helix B (R553Q) of $Kv7.2_{CT}$ differently affected CaM interaction. In fact, W344R (yellow plots) and wt$Kv7.2_{CT}$ induced an identical maximal increase of D-CaM fluorescence emission, both in the presence (Fig. 3A) and in the absence of Ca^{2+} (Fig. 3B); moreover, when compared to wt, the W344R mutation slightly but significantly increased the apparent affinity for CaM, both in the presence and in the absence of Ca^{2+} (Fig. 3; Table 1). By contrast, the L351V mutation (green plots), slightly, but significantly reduced CaM affinity, although it failed to affect maximal fluorescence intensity (Table 1). All the other tested mutations induced a significant decrease in the maximal D-CaM fluorescence emission and in CaM affinity, both in the presence and in the absence of Ca^{2+} (Fig. 3; Table 1). Reassuringly, the nanomolar apparent affinities for CaM obtained for wt and mutant $Kv7.2_{CT}$ constructs in D-CaM fluorescence measurements were very similar to those described from SPR experiments (Fig. 2C).

3.4. Mutations in the C-terminus interfere with the functional regulation of Kv7.2 channels by CaM

In order to investigate the consequences of the observed changes in CaM affinity induced by the different C-terminus mutations on Kv7.2 channel function, we developed a functional assay of CaM–dependent Kv7.2 current regulation. Expression of Kv7.2 subunits in CHO cells gave rise to typical outward K^+ currents with a threshold potential for activation of about −40 mV [22] (Fig. 4A), and a current density at 0 mV of 28.1 ± 3.4 pA/pF ($n = 12$). CaM co-expression with Kv7.2 subunits induced a dose-dependent increase of Kv7.2 current density (Fig. 4D). In fact, while a Kv7.2:CaM cDNA transfection ratio of 1:1 or 1:3 failed to modify the maximal current density ($n = 8$; $p > 0.05$ *versus* cells expressing Kv7.2), a significant increase was instead measured when a transfection ratio of 1:5 was used ($n = 30$; $p < 0.05$ *versus*

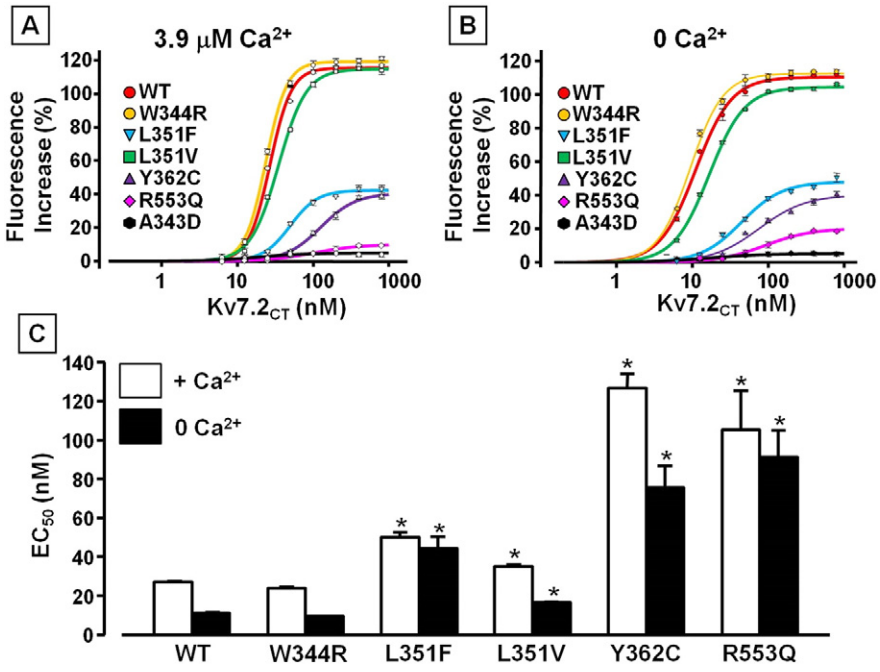

Fig. 3. Interaction between $Kv7.2_{CT}$ and CaM studied by D-CaM fluorescence. A–B) Concentration–fluorescence curves obtained by reacting 12.5 nM D-CaM with increasing concentrations of the indicated GST-fusion proteins in the presence (A) or in the absence (B; + 10 mM EGTA) of Ca^{2+}, as indicated. Data are the means ± SEM of at least 4 independent experiments and are expressed as % of the fluorescence increase measured when D-CaM was reacted with wtGST–$Kv7.2_{CT}$. C) Apparent binding affinities (EC_{50}) derived from the data shown in A (white columns) or in B (black columns). Asterisks indicate values significantly different ($p < 0.05$) versus wtGST–$Kv7.2_{CT}$.

cells expressing Kv7.2); a lower transfection ratio (Kv7.2:CaM = 1:10) failed to further enhance Kv7.2 currents. Co-expression of Kv7.2 with a mutant CaM unable to bind Ca^{2+} (CaM_{1234}; transfection ratio Kv7.2:CaM_{1234} = 1:5 or 1:10) [23], exerted even larger effects on Kv7.2 current density (n = 30; $p < 0.05$ *versus* cells expressing Kv7.2 or Kv7.2 + CaM; Fig. 4A). These results suggested that CaM-induced Kv7.2 current increase was largely independent on its Ca^{2+}-binding ability. In addition to increasing maximal current size, CaM_{1234} overexpression also caused a strong leftward shift in the voltage-dependence of activation of Kv7.2-mediated currents; by contrast, CaM only caused a small (less than 2 mV) rightward shift in Kv7.2 channels gating (Table 2).

To investigate the molecular mechanism underlying CaM- or CaM_{1234}-dependent Kv7.2 current potentiation, Western blot experiments were performed in cells in which Kv7.2 cDNA was co-transfected with CaM or CaM_{1234} cDNA. In accordance to Gamper and Shapiro [24], anti-CaM antibodies revealed a faint endogenous CaM band in untransfected cells; by contrast, stronger signals were detected by these antibodies upon CaM or CaM_{1234} cotransfection (1:5 cDNA ratio for Kv7.2 and CaM or CaM_{1234}) (Fig. 4B). Despite the identical cDNA transfection ratio, the intensity of the band corresponding to CaM_{1234} was higher than that of CaM; this might be due to true differences in the steady-state levels of the two proteins, as well as to an enhanced affinity of the anti-CaM antibodies for CaM_{1234}, as previously suggested for anti-CaM antibodies from a different commercial source [24]. Notably, biotinylation experiments revealed that CaM or CaM_{1234} overexpression failed to modify the ratio between the intensity of the OD_{Q2BIOT}/OD_{Q2TOT}, which was 1.0 ± 0.7, 1.6 ± 1.1, or 1.5 ± 0.8 in cells expressing Kv7.2, Kv7.2 + CaM, or Kv7.2 + CaM_{1234} (n = 6; $p > 0.05$; Fig. 4C), suggesting that the enhancement of Kv7.2 currents observed in electrophysiological experiments was not due to increased plasma membrane levels of Kv7.2 subunits.

When the effects of CaM or CaM_{1234} co-transfection were investigated on the functional properties of currents expressed by Kv7.2 channels carrying W344R, L351F, L351V, Y362C or R553Q BFNS-causing mutations, widely diverging effects were found (Fig. 4D). In particular, when compared to Kv7.2 channels, maximal current densities from Kv7.2–L351V channels were unchanged when expressed alone as well as upon CaM- or CaM_{1234} co-transfection. On the other hand, the W344R mutation abolished Kv7.2 currents, both in the absence and in

Table 1
Summary of the $Kv7.2_{CT}$ binding parameters obtained using 12.5 nM D-CaM.

GST–$Kv7.2_{CT}$	−Ca^{2+} (EGTA 10 mM)			+Ca^{2+} (3.9 μM)		
	Maximal fluorescence increase	EC_{50} (nM)	h (n)	Maximal fluorescence increase	EC_{50} (nM)	h (n)
WT[a]	111.0 ± 1.4	11.0 ± 0.5	1.6 ± 0.3 (6)	115.0 ± 2.1	27.1 ± 1.2	3.4 ± 0.5 (5)
W344R	113.0 ± 1.5	9.4 ± 0.4	2.1 ± 0.2 (4)	119.0 ± 0.8	23.9 ± 0.4	3.1 ± 0.1 (4)
L351V	105.0 ± 0.8	16.6 ± 0.4	1.8 ± 0.1 (4)	115.0 ± 1.2	31.9 ± 0.9	2.4 ± 0.1 (4)
L351F	48.0 ± 2.3	44.5 ± 5.9	1.6 ± 0.3 (4)	42.3 ± 0.9	50.1 ± 2.5	2.4 ± 0.3 (4)
Y362C	40.1 ± 2.3	75.6 ± 11.1	1.4 ± 0.2 (4)	40.6 ± 1.2	127.0 ± 7.5	1.9 ± 0.1 (4)
R553Q	20.1 ± 1.2	91.3 ± 13.7	1.4 ± 0.3 (4)	10.3 ± 0.8	105.0 ± 21.0	1.4 ± 0.3 (4)
A343D[a]	5.3 ± 0.3	N.D.	N.D. (4)	4.8 ± 0.3	N.D.	N.D. (4)

h = Hill coefficient.
(n) = number of independent experiments.
EC_{50} = concentration producing 50% of the maximal effect.
N.D. = not determined.
[a] Data from Alaimo and coll. [31].

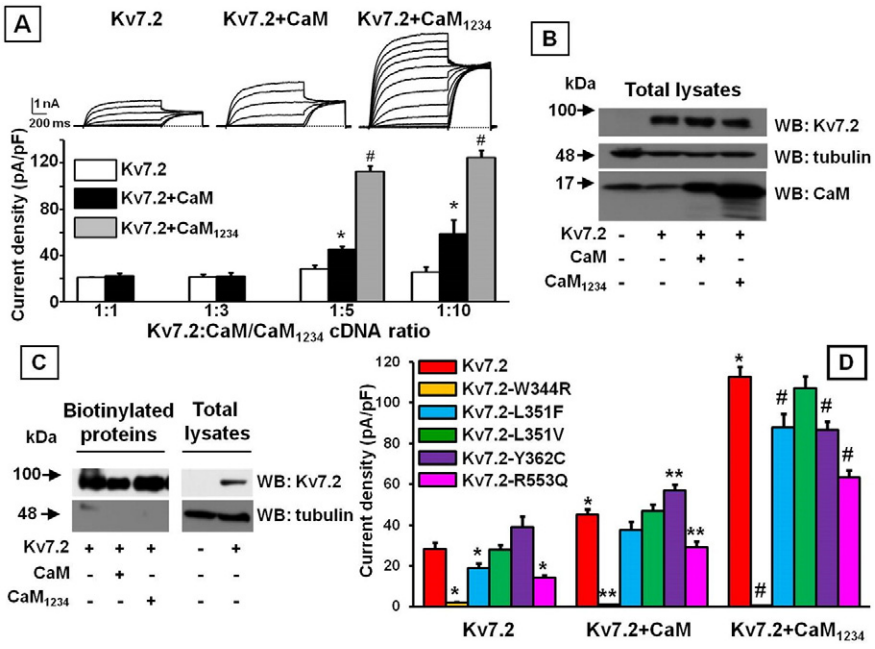

Fig. 4. Effect of BFNS-causing mutations on CaM-dependent modulation of Kv7.2 homomeric channels. A) Concentration-dependent increase of Kv7.2 current density (measured at 0 mV) by CaM (black bars) or CaM_{1234} (gray bars) coexpression at different cDNAs ratio (from 1:1 to 1:10), as reported. Representative current traces measured in response to the indicated voltage protocol in cells expressing Kv7.2, Kv7.2 + CaM or Kv7.2 + CaM_{1234} (cDNA transfection ratio Kv7.2:CaM = 1:5) are shown in the inset. B–C) Representative image of Western-blotting experiments performed on total lysates (B) or biotinylated fractions (C) of CHO cells expressing Kv7.2, Kv7.2 + CaM, or Kv7.2 + CaM_{1234}, as indicated (cDNA transfection ratio Kv7.2:CaM = 1:5). The arrows and the numbers on the left of each image indicate the position of the protein marker. D) Quantification of the current densities measured at 0 mV in CHO cells expressing wt or mutant Kv7.2 channels alone (group of bars on the left; *data from* [22]), or co-expressing CaM (group of bars in the middle) or CaM_{1234} (group of bars on the right). * = $p < 0.05$ versus Kv7.2; ** = $p < 0.05$ versus Kv7.2 + CaM; # = $p < 0.05$ versus Kv7.2 + CaM_{1234}.

the presence of CaM or CaM_{1234}. The other mutants displayed a somehow more complex behavior. In fact, Kv7.2–L351F and Kv7.2–R553Q channels, both showing reduced maximal current densities in the absence of exogenous CaM, were significantly potentiated by CaM or CaM_{1234} co-expression. With CaM, the extent of current potentiation in both these mutants appeared larger when compared to Kv7.2 channels; in fact, the percent of current increase by CaM was 60.7 ± 9.5%, 118.7 ± 21.3%, or 103.7 ± 21.0%, for Kv7.2, Kv7.2–L351F, or Kv7.2–R553Q channels, respectively ($p < 0.05$ *versus* Kv7.2), leading to a complete (L351F) or partial (R553Q) restoration of wild-type current levels. By contrast, with CaM_{1234}, the percent of current increase were identical in Kv7.2, Kv7.2–L351F, or Kv7.2–R553Q channels (being 399.9 ± 17.5%, 463.8 ± 34.8% or 443.5 ± 23.7%, for Kv7.2, Kv7.2–L351F, or Kv7.2–R553Q channels, respectively), and the maximal current density for both these mutants upon CaM_{1234} co-transfection was still smaller than that of wt channels. In the case of the Y362C mutant, whose current density was similar to that of Kv7.2 channels when expressed alone, currents recorded in CaM- or CaM_{1234}-co-expressing cells were larger or smaller, respectively, than those of wt channels. As for wt channels, CaM_{1234} co-expression caused a significant leftward shift in

Table 2
Biophysical properties of wild-type or mutant Kv7.2 channels, in homomeric or heteromeric configuration with Kv7.3 subunits, upon CaM or CaM_{1234} over-expression.

Channel	*n*	Control		+ CaM		+ CaM_{1234}	
		$V_{1/2}$ (mV)	*k* (mV/efold)	$V_{1/2}$ (mV)	*k* (mV/efold)	$V_{1/2}$ (mV)	*k* (mV/efold)
Kv7.2	26–28	−21.3 ± 0.6	12.6 ± 0.5	−19.2 ± 0.5*	12.4 ± 0.5	−34.7 ± 0.9*,**	13.3 ± 0.7
Kv7.2–L351F	17–32	−22.1 ± 0.6	13.3 ± 0.7	−20.9 ± 0.8	13.3 ± 0.7	−33.3 ± 0.6*,**	12.5 ± 0.5
Kv7.2–L351V	22–29	−24.1 ± 0.5$^{\#}$	11.1 ± 0.5	−23.2 ± 0.8$^{\#\#}$	12.2 ± 0.6	−30.9 ± 0.6$^{*,**,\#\#\#}$	13.4 ± 0.5
Kv7.2–Y362C	21–30	−24.3 ± 1.0$^{\#}$	12.3 ± 0.9	−23.3 ± 0.6$^{\#\#}$	11.8 ± 0.5	−28.2 ± 0.6$^{*,**,\#\#\#}$	12.0 ± 0.5
Kv7.2–R553Q	17–21	−20.6 ± 0.6	11.5 ± 0.6	−22.9 ± 0.7$^{\#\#}$	13.8 ± 0.6	−28.4 ± 1.1$^{*,**,\#\#\#}$	14.1 ± 0.9
Kv7.3	12–14	−36.9 ± 0.4$^{\#}$	5.9 ± 0.3$^{\#}$	−37.4 ± 0.5	6.2 ± 0.4	−37.9 ± 0.6	6.7 ± 0.5
Kv7.2/Kv7.3	21–24	−28.7 ± 0.3$^{\#,\circ}$	11.2 ± 0.3$^{\#,\circ}$	−30.4 ± 0.3*	11.4 ± 0.3	−38.0 ± 0.5**	11.3 ± 0.4
Kv7.2/Kv7.2–W344R/Kv7.3	14–22	−29.7 ± 0.4	9.6 ± 0.3	−29.0 ± 0.4	9.9 ± 0.3	−36.5 ± 0.4*,**	10.4 ± 0.3
Kv7.2/Kv7.2–L351F/Kv7.3	20–22	−28.5 ± 0.4	10.3 ± 0.3	−28.0 ± 0.3	10.8 ± 0.3	−35.3 ± 0.5*,**,†	12.1 ± 0.4**
Kv7.2/Kv7.2–L351V/Kv7.3	18–21	−28.9 ± 0.4	10.7 ± 0.4	−29.9 ± 0.4	11.0 ± 0.4	−37.3 ± 0.5*,**	10.9 ± 0.4
Kv7.2/Kv7.2–Y362C/Kv7.3	16–22	−31.0 ± 0.4$^{\$}$	11.0 ± 0.3	−30.1 ± 0.4	11.1 ± 0.3	−34.9 ± 0.4*,**,†	11.2 ± 0.4
Kv7.2/Kv7.2–R553Q/Kv7.3	18–21	−28.9 ± 0.3	10.5 ± 0.3	−29.6 ± 0.3	10.6 ± 0.3	−35.1 ± 0.5*,**,†	11.2 ± 0.4

* $p < 0.05$ versus respective controls without CaM.
** $p < 0.05$ versus respective controls with CaM.
$^{\#}$ $p < 0.05$ versus Kv7.2.
$^{\#\#}$ $p < 0.05$ versus Kv7.2 + CaM.
$^{\#\#\#}$ $p < 0.05$ versus Kv7.2 + CaM_{1234}.
$^{\circ}$ $p < 0.05$ versus Kv7.3.
$^{\$}$ $p < 0.05$ versus Kv7.2 + Kv7.3.
† $p < 0.05$ versus Kv7.2 + Kv7.3 + CaM_{1234}.

the voltage-dependence of activation for each mutant Kv7.2 channel; by contrast, no change was measured when CaM was overexpressed (Table 2).

To mimic the genetic condition of the individuals affected with BFNS who carry a single mutant Kv7.2 allele, we also performed electrophysiological recordings in CHO cells expressing mutant subunits in Kv7.2/Kv7.3 heteromers, together with CaM or CaM_{1234}. As previously reported [5], Kv7.2 co-expression with Kv7.3 (transfection ratio 1:1, using 0.3 + 0.3 μg of cDNA) caused a significant increase in the maximal current density (Fig. 5) and a leftward shift in the voltage dependence of activation (Table 2) when compared to Kv7.2 homomeric channels. Furthermore, CaM or CaM_{1234} over-expression together with Kv7.2/Kv7.3 heteromeric channels (transfection ratio 1:1:10, using 0.3 + 0.3 + 3 μg of cDNA) increased current density (Fig. 5) and promoted a leftward shift in the voltage-dependence of activation (Table 2). By contrast, CaM or CaM_{1234} failed to modify Kv7.3 current size (current densities were 12.4 ± 3.2, 10.1 ± 3.4, 19.9 ± 4.2 pA/pF, for Kv7.3, Kv7.3 + CaM or Kv7.3 + CaM_{1234}, respectively; n = 18–26; $p > 0.05$ among each other) or activation voltage-dependence (Table 2), suggesting that Kv7.2/Kv7.3 CaM-mediated modulation is strongly dependent on the presence of Kv7.2 subunits.

As previously reported [22], when Kv7.2–L351V or Kv7.2–Y362C subunits were co-expressed with Kv7.2/Kv7.3 channels (transfection ratio 0.5:0.5:1, using 0.15 + 0.15 + 0.3 μg of cDNA), no significant change was measured in terms of maximal current density (Fig. 5); in cells expressing these channels, co-transfection with CaM or CaM_{1234} increased current levels and modified gating in a similar fashion as in Kv7.2/Kv7.3 channels (Fig. 5; Table 2). By contrast, while we previously reported a reduction in maximal currents when Kv7.2–W344R subunits were expressed together with Kv7.2/Kv7.3 subunits [22], we failed to detect any significant change in the present experiments (Fig. 5; Table 2). However, in the present study, smaller amounts of Kv7.2/Kv7.3 cDNAs were transfected (total of 0.6 μg instead of 3 μg used in the previous study) to allow for the co-transfection of a 5-fold higher amount (3 μg) of CaM cDNA. These results suggest that Kv7.2–W344R mutant subunits-induced suppression of Kv7.2/Kv7.3 heteromeric channel function strictly depends on the amount of cDNA transfected. By contrast, L351F or R553Q mutations decreased heteromeric maximal current density (Fig. 5), without affecting the voltage-dependence of activation (Table 2). In cells expressing these channels, CaM over-expression (transfection ratio 0.5:0.5:1:10, using 0.15 + 0.15 + 0.3 + 3 μg of cDNA) fully restored current density to control levels in heteromeric channels carrying Kv7.2–L351F or Kv7.2–R553Q mutant subunits. Instead, CaM_{1234} over-expression only partially restored channel function, and promoted a leftward shift in the voltage-dependence of activation (Table 2).

4. Discussion

The KCNQ2 gene is a major locus for BFNS, and studies in heterologous expression systems and in mice models converge on the hypothesis that a decrease in I_{KM} function (underlied by KCNQ2-encoded Kv7.2 subunits) is sufficient to cause BFNS, therefore indicating haploinsufficiency as a primary pathogenetic mechanism for both familial and sporadic BFNS cases [39]. Two main general mechanisms can account for mutation-induced decrease in Kv7.2 currents: defects in voltage-sensing mostly caused by mutations affecting the S_1–S_4 voltage-sensing domain [8,40,41], and defective subunit stability [42] and trafficking [32], subcellular targeting [43], or regulation by intracellularly-acting modulators [22,44] for those mutations affecting the long intracellular C-terminal domain. In Kv7 channels, this region provides attachment sites for several regulatory molecules [34,35]; among these, CaM binds to two non-continuous α helical regions (called A and B helices) [14]. In the present work, recently described BFNS-causing mutations [22] falling in Kv7.2 C-terminus helix A (W344R, L351F, L351V), helix B (R553Q), or A–B inter-helical region (Y362C) have been investigated with respect to their ability to affect CaM binding and CaM-dependent Kv7.2 or Kv7.2/Kv7.3 functional modulation.

To this aims, Kv7.2/CaM interaction has been studied by semi-quantitative (Far-Western blotting experiments) and quantitative (D-CaM fluorescence and SPR assays) biochemical approaches. For these experiments, a large amount of CaM was easily purified in native configuration. Instead, Kv7.2 C-terminal fragments were much more difficult to purify because of their marked tendency to aggregate; therefore, they were either extracted from inclusion bodies from total

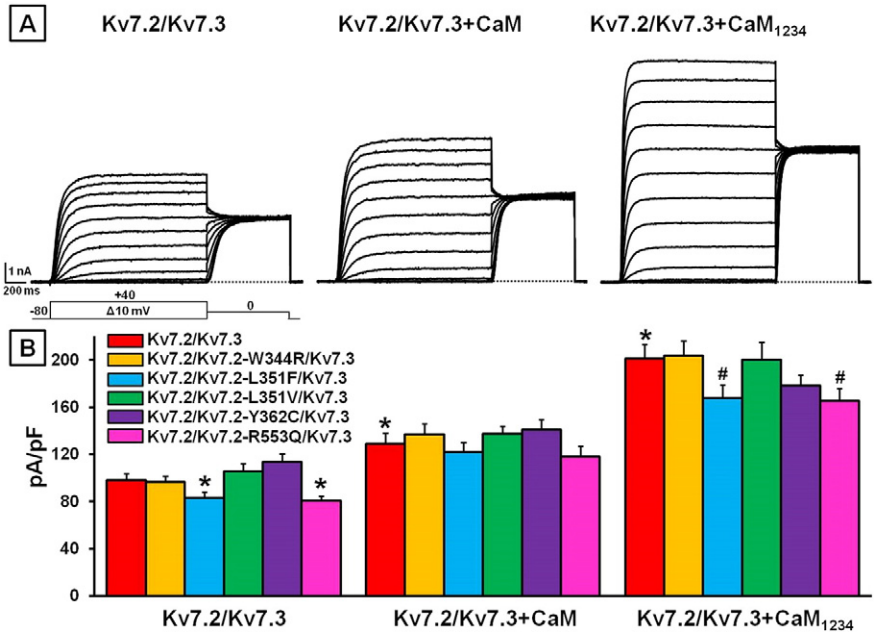

Fig. 5. Effect of BFNS-causing mutations on CaM-dependent modulation of Kv7.2/Kv7.3 heteromeric channels. A) Representative current traces measured in response to the indicated voltage protocol in cells expressing Kv7.2/Kv7.3, Kv7.2/Kv7.3 + CaM or Kv7.2/Kv7.3 + CaM_{1234} (transfection ratio 1:1, using 0.3 + 0.3 μg of cDNA for Kv7.2/Kv7.3; transfection ratio 1:1:10, using 0.3 + 0.3 + 3 μg of cDNA for Kv7.2/Kv7.3 + CaM or Kv7.2/Kv7.3 + CaM_{1234}). B) Quantification of the current densities measured at 0 mV in CHO cells expressing wt or mutant Kv7.2/Kv7.3 channels in the absence or in the presence of co-expressed CaM or CaM_{1234}, as indicated. * = $p < 0.05$ versus Kv7.2/Kv7.3; # = $p < 0.05$ versus Kv7.2/Kv7.3 + CaM_{1234}.

bacterial lysates using denaturation/renaturation steps (as in D-CaM fluorescence measurements) or used without any purification procedure to preserve maximal protein activity (as in Far-Western blotting and SPR experiments, both requiring larger protein amounts). Since CaM-mediated target protein regulation is often dependent on $[Ca^{2+}]_i$ [45,46], D-CaM experiments were performed both in the presence and in the absence of Ca^{2+}; by contrast, technical limitations impeded the evaluation of Kv7.2 affinity for CaM in the absence of Ca^{2+} in SPR experiments. Nevertheless, the similarity in CaM affinities when these were measured for each Kv7.2 C-terminal construct in the presence of Ca^{2+} by two very different techniques, namely D-CaM fluorescence and SPR experiments, is strongly suggestive of the biological relevance of the observed differences. This view was also confirmed by the fact that, using all three experimental approaches (Far-Western blotting, SPR, and D-CaM fluorescence), CaM binding was abolished or strongly diminished by the A343D mutation in helix A, as previously demonstrated [32,36]. The biochemical results obtained suggest that CaM binds to Kv7.2 C-terminus with higher affinity in the absence of Ca^{2+}. The W344R mutation failed to affect CaM binding, either in the presence or in the absence of Ca^{2+}; a similar pattern was also observed with the L351V mutation, although this substitution slightly (but significantly) reduced CaM affinity both in the presence and in the absence of Ca^{2+}. By contrast, the L351F, Y362C, and R553Q mutations significantly reduced CaM affinity in the presence or absence of Ca^{2+}; in the case of the L351F and R553Q, identical CaM affinities were observed both in the presence and in the absence of the divalent cation.

To evaluate the functional consequences of the mutation-induced altered CaM binding revealed by biochemical experiments, an assay for CaM-dependent Kv7.2 current regulation was developed. In fact, we found that Kv7.2 currents were potentiated in a dose-dependent manner by CaM overexpression; an even stronger current enhancement was observed upon Kv7.2 co-expression with CaM_{1234}, a CaM isoform unable to bind Ca^{2+} [23]. CaM binding has been shown to play a crucial role in the export from the endoplasmic reticulum and plasma membrane expression of Kv7.2 channels expressed in HEK cells [36], and for polarized axonal surface expression of Kv7.2 subunits in rat hippocampal neurons [44]. Furthermore, CaM binding to the C-terminus regulates Kv7.2 assembly with Kv7.3, thus influencing expression of heteromeric channels at the axon initial segment [47]. In our experiments, we tested whether the observed CaM-induced current potentiation was related to an increase in plasma membrane expression of Kv7.2 subunits using membrane protein biotinylation. The results obtained suggested that CaM- or CaM_{1234}-induced Kv7.2 current potentiation could not be accounted for by an increase in plasma membrane trafficking of channel subunits. Rather, given that CaM is unlikely to influence the single channel conductance, an effect on the opening probability, mainly regulated by PIP_2 affinity [13] appears as a likely explanation. The observed difference between CaM and CaM_{1234} in Kv7.2 current potentiation could be attributed to the fact that, while Ca^{2+}-unbound CaM (apo-CaM) appears mainly to play a permissive role on channel open state [45], Ca^{2+}-CaM (holo-CaM) mediates inhibitory signals [24], preferentially inducing channel closure [48]. The ability of CaM (and of apo-CaM, in particular) to regulate channel gating is consistent with recent results obtained with CaM proteins chemically derivatized with tethered pore blockers of different lengths, showing that the CaM binding site is positioned rather close to the cytoplasmic gate of Kv7.2 channels [49]. Consistent with this view is also the present observation that CaM_{1234}, but not CaM, overexpression, beside increasing the maximal current density, also prompted a robust leftward shift in the voltage-dependence of activation of Kv7.2 and Kv7.2/Kv7.3 currents, indicative of an increased sensitivity to voltage of the opening process. Previous reports suggested that CaM (but not CaM_{1234}) overexpression reduced Kv7.2 maximal current density [50]; differences in the electrophysiological recording technique (whole-cell or perforated patch-mode), in the intracellular solution composition (EGTA concentrations, in particular), and in Kv7.2:CaM co-transfected cDNA ratios could explain this discrepancy. In addition, differences in the Kv7.2 splice variants diverging in the A–B linker might also provide a plausible explanation; in fact, while isoform c has been used in present experiments, those from Gamper and Shapiro [50] were instead performed with isoform d (GenBank accession no. AF_110020). As a matter of fact, splice variant-dependent current modulation by CaM_{1234} (but not by CaM) has been described in closely-related Kv7.4 channels [51].

Using the described functional assay, it was found that the W344R mutation, despite binding CaM with wt affinity, did not express functional currents when expressed homomerically [22], also when co-expressed with CaM or CaM_{1234}. These results suggested that the W344 residue is involved in the structural rearrangements translating CaM binding into pore gating, therefore playing a critical role in favoring channel opening upon CaM binding, and revealing that CaM binding is essential, but not sufficient for pore opening. The presence of an aromatic side chain at the W344 position, despite being dispensable for CaM binding, is strictly required for Kv7.2 channel function [22], and an aromatic residue is often found at the corresponding position in the IQ CaM-binding motif in many CaM target proteins [46]. By contrast, all the other previously-studied mutations in helix A reduced CaM binding to Kv7.2 [36], and abolished (I340E, A343D) or strongly reduced (R353G, another mutation found in a BFNS family; [52]) Kv7.2 currents.

On the other hand, currents expressed by L351F– or R553Q–Kv7.2 mutant channels, which were smaller than those carried by wt channels when expressed alone, were consistently increased by CaM- or CaM_{1234} overexpression. In CaM-co-expressing cells, the extent of current potentiation in both Kv7.2–L351F or Kv7.2–R553Q mutants was larger than in wt channels, leading to a full (in the case of L351F) or an almost complete (for R553Q) normalization of the maximal current density; these results suggest that the reduced size of the currents expressed by Kv7.2 channels carrying each of these mutants in the absence of added CaM can be attributed to a mutation-dependent reduction in CaM affinity. The results obtained are qualitatively similar to those described for other mutations in the A (I340A; [31]) or B (S539D; corresponding to the S511D reported in the splice variant studied by Alaimo and coll. [31]) helix which failed to carry significant currents when expressed alone, but were rescued by CaM or CaM_{1234} co-expression. Structural studies have revealed that the residue corresponding to R553 in highly-homologous Kv7.4 subunits is involved in electrostatic interactions with CaM [48]; the pathophysiological relevance of such finding seems also supported by the observation that the Kv7.2–R553 residue immediately precedes another positively charged, CaM-interacting residue [48], which has been found mutated in an atypical BFNS-affected family (K554N; [53]). Noteworthy, non-aromatic side chain at the L351 position seems to be an important structural requirement for proper CaM-induced regulation of Kv7.2 channel function; in fact, the L351V substitution, opposite to the more disruptive L351F substitution, only slightly reduced Kv7.2 affinity for both CaM and CaM_{1234}, and displayed a neutral behavior in our functional tests.

Finally, the Y362C mutation, which did not alter steady-state Kv7.2 current levels in control condition, reduced CaM affinity in biochemical experiments and affected CaM- and CaM_{1234}-induced current regulation in electrophysiological experiments, suggesting that a reduced affinity *versus* CaM is not predictive *per se* of a decrease in Kv7.2 currents. This result is similar to that obtained for Kv7.2 channels carrying another mutation (C527R), showing altered CaM binding, but normal current levels [45]. It should be underlined that the Y362 residue falls within the A–B interhelical region, and recent structural insights in the highly homologous Kv7.1 channel reveal that this region is unlikely to contribute to CaM binding [54]. However, it has been recently suggested that the A–B linker influences PIP_2 affinity [19], and that an interplay between CaM binding and PIP_2 affinity regulates muscarinic-induced suppression of Kv7.2 channels [55]. Thus, we suggest that, in this mutant, changes in PIP_2 affinity could counterbalance the functional effects caused by the reduced CaM affinity.

To further explore the pathophysiological relevance of these findings for BFNS patients, who carry a single Kv7.2 mutated allele, we also studied

the effects of CaM over-expression on heteromeric channels reproducing the Kv7.2/Kv7.3 genetic balance found in BFNS individuals. The results obtained suggest that the reduction in current size observed in heteromeric Kv7.2/Kv7.3 channels incorporating Kv7.2–L351F or Kv7.2–R553Q mutant subunits was fully reversed by CaM over-expression; instead, in both these mutants, CaM_{1234} overexpression, although strongly enhancing channel function, failed to restore current levels to control values. No functional difference was observed in the case of the W344R, L351V, and Y362C mutations between control and CaM- (or CaM_{1234}) transfected cells. Thus, mainly quantitative differences occurred in CaM- or CaM_{1234}-induced regulation when Kv7.2 mutant subunits are incorporated into homomers or into heteromeric channels with Kv7.2 and Kv7.3 subunits. Particularly striking is the behavior of the W344R mutation, which generated non-functional channels when expressed in homomeric configuration, but failed to interfere with the currents carried by Kv7.2/Kv7.3 subunits. Thus, although additional studies are needed to better elucidate the pathogenic mechanism by which this mutation is epileptogenic in humans, changes in CaM affinity appear unlikely.

Noteworthy, the changes in CaM-dependent Kv7.2 modulation prompted by some of the BFNS-associated mutations herein described cannot be considered exhaustive of the complex possible mechanisms by which these mutations affect Kv7.2 channel function. Noteworthy, the same mutations also interfere with the functional regulation by syntaxin-1A [22], a member of the soluble N-ethylmaleimide-sensitive-factor attachment protein receptor (SNARE) complex, which downregulates Kv7.2 channel gating by binding to a site on Kv7.2 channels largely overlapping that of CaM [16]. A further study from the same group [21] also reported that co-expression of CaM with syntaxin increased CaM binding to Kv7.2, although it fully blocked the inhibitory effect of syntaxin on Kv7.2 current amplitude; in their experiments, these Authors also showed by fluorescence resonance energy transfer experiments that the functional changes produced by CaM on channel gating are accompanied by an increased proximity between the N- and C-termini. The ability of Kv7.2 mutations to interfere with both CaM- (this study) and syntaxin- [22] induced functional regulation is suggestive of a potentially competitive interaction between these two regulators involving the C-terminal region, although further studies are needed to confirm such an hypothesis. Furthermore, it should be considered that other regulatory pathways (including PKC phosphorylation or PIP_2 binding), also acting at the same C-terminal region, could be affected by these mutations.

It should be pointed out that, in the present experiments, the consequences of the mutations on CaM binding have been investigated using Kv7.2 C-terminal fragments rather than the full-length channel subunit; thus, the correlation between biochemical and functional results must be viewed with caution. We carried out several attempts in co-immunoprecipitation experiments with different Kv7.2 and CaM constructs and antibodies, but severe technical limitations precluded a precise quantification of the affinity between the two interacting proteins (data not shown). Nevertheless, despite such potential limitation, each of the BFNS-causing mutations in Kv7.2 C-terminal region herein investigated appear to prompt specific biochemical and/or functional consequences, ranging from slight alterations in CaM affinity which did not translate into functional changes (L351V), to a significant reduction in the affinity and functional modulation by CaM (L351F, Y362C or R553Q), to a complete abolishment of functional behavior without significant alteration in CaM affinity (W344R). In Kv7.2–L351F and Kv7.2–R553Q mutants, CaM overexpression restored normal Kv7.2 or Kv7.2/Kv7.3 channel function.

Altogether, the present results further our knowledge of the complex molecular network regulating Kv7.2 channels, provide a rationale pathogenetic mechanism for mutation-induced Kv7.2 channel dysfunction in BFNS, and highlight CaM-dependent Kv7.2 current enhancement as a potential therapeutic approach in Kv7.2-related epilepsies.

Supplementary data to this article can be found online at http://dx.doi.org/10.1016/j.bbadis.2015.06.012.

Acknowledgments

A. Alaimo was supported by the Fundación Biofísica Bizkaia and by Universidad del País Vasco (UPV/EHU) postdoctoral fellowship. A. Alberdi holds a JAE-predoctoral CSIC fellowship co-financed with European Social Funds (JAEPre_2010_00711). M. V. Soldovieri is supported by a Postdoctoral fellowship from the Italian Society for Pharmacology. This work was supported in part by grants from the Spanish Ministry of Economy and Competitiveness (BFU2012-39883), the Spanish Ion Channel Initiative Consolider project (CSD2008-00005), and the Basque Government (SAIOTEK SA-2006/00023 and 304211ENA9) to AV; and by grants from Telethon (GGP07125), the Fondazione San Paolo — IMI (Project Neuroscience), Regione Molise (Convenzione AIFA/Regione Molise), and the Science and Technology Council of the Province of Avellino to MT.

References

[1] N.A. Singh, C. Charlier, D. Stauffer, B.R. DuPont, R.J. Leach, R. Melis, G.M. Ronen, I. Bjerre, T. Quattlebaum, J.V. Murphy, M.L. McHarg, D. Gagnon, T.O. Rosales, A. Peiffer, V.E. Anderson, M. Leppert, A novel potassium channel gene, KCNQ2 is mutated in a inherited epilepsy of newborns, Nat. Genet. 18 (1998) 25–29.
[2] C. Biervert, B.C. Schroeder, C. Kubisch, S.F. Berkovic, P. Propping, T.J. Jentsch, O.K. Steinlein, A potassium channel mutation in neonatal human epilepsy, Science 279 (1998) 403–406.
[3] G. Bellini, F. Miceli, M.V. Soldovieri, E. Miraglia del Giudice, G. Coppola, M. Taglialatela, KCNQ2-Related Disorders, in: R.A. Pagon, M.P. Adam, H.H. Ardinger, T.D. Bird, C.R. Dolan, C.T. Fong, R.J.H. Smith, K. Stephens (Eds.), GeneReviews® [Internet], Seattle (WA), University of Washington, Seattle, 2010 (updated 2013 Apr 11).
[4] S. Weckhuysen, S. Mandelstam, A. Suls, D. Audenaert, T. Deconinck, L.R. Claes, L. Deprez, K. Smets, D. Hristova, I. Yordanova, A. Jordanova, B. Ceulemans, A. Jansen, D. Hasaerts, F. Roelens, L. Lagae, S. Yendle, T. Stanley, S.E. Heron, J.C. Mulley, S.F. Berkovic, I.E. Scheffer, P. de Jonghe, KCNQ2 encephalopathy: emerging phenotype of a neonatal epileptic encephalopathy, Ann. Neurol. 71 (2012) 15–25.
[5] H.S. Wang, Z. Pan, W. Shi, B.S. Brown, R.S. Wymore, I.S. Cohen, J.E. Dixon, D. McKinnon, KCNQ2 and KCNQ3 potassium channel subunits: Molecular correlates of the M-channel, Science 282 (1998) 1890–1893.
[6] N.V. Marrion, Control of M-current, Annu. Rev. Physiol. 59 (1997) 483–504.
[7] C.C. Hernandez, O. Zaika, G.P. Tolstykh, M.S. Shapiro, Regulation of neural KCNQ channels: signalling pathways, structural motifs and functional implications, J. Physiol. 586 (2008) 1811–1821.
[8] M.V. Soldovieri, M.R. Cilio, F. Miceli, G. Bellini, E. Miraglia del Giudice, P. Castaldo, C.C. Hernandez, M.S. Shapiro, A. Pascotto, L. Annunziato, M. Taglialatela, Atypical gating of M-type potassium channels conferred by mutations in uncharged residues in the S4 region of KCNQ2 causing Benign Familial Neonatal Convulsions, J. Neurosci. 27 (2007) 4919–4928.
[9] F. Miceli, M.V. Soldovieri, C.C. Hernandez, M.S. Shapiro, L. Annunziato, M. Taglialatela, Gating consequences of charge neutralization of arginine residues in the S4 segment of Kv7.2, an epilepsy-linked K^+ channel subunit, Biophys. J. 95 (2008) 2254–2264.
[10] F. Miceli, M.V. Soldovieri, L. Lugli, G. Bellini, P. Ambrosino, M. Migliore, E. Miraglia del Giudice, F. Ferrari, A. Pascotto, M. Taglialatela, Neutralization of a unique, negatively-charged residue in the voltage sensor of Kv7.2 subunits in a sporadic case of Benign Familial Neonatal Seizures, Neurobiol. Dis. 34 (2009) 501–510.
[11] M. Schwake, T.J. Jentsch, T. Friedrich, A carboxy-terminal domain determines the subunit specificity of KCNQ K^+ channel assembly, EMBO Rep. 4 (2003) 76–81.
[12] R.J. Howard, K.A. Clark, J.M. Holton, D.L. Minor, Structural insight into KCNQ (Kv7) channel assembly and channelopathy, Neuron 53 (2007) 663–675.
[13] Y. Li, N. Gamper, D.W. Hilgemann, M.S. Shapiro, Regulation of K_V7 (KCNQ) K^+ channel open probability by phosphatidylinositol 4,5-bisphosphate, J. Neurosci. 25 (2005) 9825–9835.
[14] E. Yus-Nájera, I. Santana-Castro, A. Villarroel, The identification and characterization of a noncontinuous calmodulin-binding site in non-inactivating voltage-dependent KCNQ potassium channels, J. Biol. Chem. 277 (2002) 28545–28553.
[15] H. Wen, I.B. Levitan, Calmodulin is an auxiliary subunit of KCNQ2/3 potassium channels, J. Neurosci. 22 (2002) 7991–8001.
[16] N. Regev, N. Degani-Katzav, A. Korngreen, A. Etzioni, S. Siloni, A. Alaimo, D. Chikvashvili, A. Villarroel, B. Attali, I. Lotan, Selective interaction of syntaxin 1A with KCNQ2: possible implications for specific modulation of presynaptic activity, PLoS One 4 (2009) e6586.
[17] N. Hoshi, J.S. Zhang, M. Omaki, T. Takeuchi, S. Yokoyama, N. Wanaverbecq, L.K. Langeberg, Y. Yoneda, J.D. Scott, D.A. Brown, H. Higashida, AKAP150 signaling complex promotes suppression of the M-current by muscarinic agonists, Nat. Neurosci. 6 (2003) 564–571.
[18] Z. Pan, T. Kao, Z. Horvath, J. Lemos, J.Y. Sul, S.D. Cranstoun, V. Bennett, S.S. Scherer, E.C. Cooper, A common ankyrin-G-based mechanism retains KCNQ and NaV channels at electrically active domains of the axon, J. Neurosci. 26 (2006) 2599–2613.
[19] C.C. Hernandez, O. Zaika, M.S. Shapiro, A carboxy-terminal inter-helix linker as the site of phosphatidylinositol 4,5-bisphosphate action on Kv7 (M-type) K^+ channels, J. Gen. Physiol. 132 (2008) 361–381.

[20] M. Bal, J. Zhang, C.C. Hernandez, O. Zaika, M.S. Shapiro, Ca^{2+}/calmodulin disrupts AKAP79/150 interactions with KCNQ (M-Type) K^+ channels, J. Neurosci. 30 (2010) 2311–2323.
[21] A. Etzioni, S. Siloni, D. Chikvashvilli, R. Strulovich, D. Sachyani, N. Regev, D. Greitzer-Antes, J.A. Hirsch, I. Lotan, Regulation of neuronal M-channel gating in an isoform-specific manner: functional interplay between calmodulin and syntaxin 1A, J. Neurosci. 31 (2011) 14158–14171.
[22] M.V. Soldovieri, N. Boutry-Kryza, M. Milh, D. Doummar, B. Heron, E. Bourel, P. Ambrosino, F. Miceli, M. De Maria, N. Dorison, S. Auvin, B. Echenne, J. Oertel, A. Riquet, L. Lambert, M. Gerard, A. Roubergue, A. Calender, C. Mignot, M. Taglialatela, G. Lesca, Novel KCNQ2 and KCNQ3 mutations in a large cohort of families with benign neonatal epilepsy: first evidence for an altered channel regulation by syntaxin-1A, Hum. Mutat. 35 (2014) 356–367.
[23] J.R. Geiser, D. van Tuinen, S.E. Brockerhoff, M.M. Neff, T.N. Davis, Can calmodulin function without binding calcium? Cell 65 (1991) 949–959.
[24] N. Gamper, M.S. Shapiro, Calmodulin mediates Ca^{2+}-dependent modulation of M-type K^+ channels, J. Gen. Physiol. 122 (2003) 17–31.
[25] F. Miceli, M.V. Soldovieri, P. Ambrosino, V. Barrese, M. Migliore, M.R. Cilio, M. Taglialatela, Genotype-phenotype correlations in neonatal epilepsies caused by mutations in the voltage sensor of K(v)7.2 potassium channel subunits, Proc. Natl. Acad. Sci. U. S. A. 110 (2013) 4386–4391.
[26] F. De Bernardis, H. Liu, R. O'Mahony, R. La Valle, S. Bartollino, S. Sandini, S. Grant, N. Brewis, I. Tomlinson, R.C. Basset, J. Holton, I.M. Roitt, A. Cassone, Human domain antibodies against virulence traits of Candida albicans inhibit fungus adherence to vaginal epithelium and protect against experimental vaginal candidiasis, J. Infect. Dis. 195 (2007) 149–157.
[27] D.G. Drescher, N.A. Ramakrishnan, M.J. Drescher, Surface Plasmon Resonance (SPR) analysis of binding interactions of proteins in inner-ear sensory epithelia, Methods Mol. Biol. 493 (2009) 323–343.
[28] Y. Wu, Q. Li, X.Z. Chen, Detecting protein–protein interactions by Far western blotting, Nat. Protoc. 2 (2007) 3278–3284.
[29] A. Camperchioli, M. Mariani, S. Bartollino, L. Petrella, M. Persico, N. Orteca, G. Scambia, S. Shahabi, C. Ferlini, C. Fattorusso, Investigation of the Bcl-2 multimerisation process: structural and functional implications, Biochim. Biophys. Acta 1813 (2011) 850–857.
[30] L.C. Russo, A.F. Asega, L.M. Castro, P.D. Negraes, L. Cruz, F.C. Gozzo, H. Ulrich, A.C. Camargo, V. Rioli, E.S. Ferro, Natural intracellular peptides can modulate the interactions of mouse brain proteins and thimet oligopeptidase with 14-3-3ε and calmodulin, Proteomics 12 (2012) 2641–2655.
[31] A. Alaimo, A. Alberdi, C. Gomis-Perez, J. Fernandez-Orth, J.C. Gomez-Posada, P. Areso, A. Villarroel, Cooperativity between calmodulin-binding sites in Kv7.2 channels, J. Cell Sci. 126 (2013) 244–253.
[32] A. Alaimo, J.C. Gómez-Posada, P. Aivar, A. Etxeberría, J.A. Rodriguez-Alfaro, P. Areso, A. Villarroel, Calmodulin activation limits the rate of KCNQ2 K^+ channel exit from the endoplasmic reticulum, J. Biol. Chem. 284 (2009) 20668–20675.
[33] A. Alaimo, C. Malo, K. Aloria, O. Millet, P. Areso, A. Villarroel, The use of dansyl-calmodulin to study interactions with channels and other proteins, Methods Mol. Biol. 998 (2013) 217–231.
[34] Y. Haitin, B. Attali, The C-terminus of Kv7 channels: a multifunctional module, J. Physiol. 586 (2008) 1803–1810.
[35] M.V. Soldovieri, F. Miceli, M. Taglialatela, Driving with no brakes: molecular pathophysiology of Kv7 potassium channels, Physiology (Bethesda) 26 (2011) 365–376.
[36] A. Etxeberria, P. Aivar, J.A. Rodriguez-Alfaro, A. Alaimo, P. Villacé, J.C. Gómez-Posada, P. Areso, A. Villarroel, Calmodulin regulates the trafficking of KCNQ2 potassium channels, FASEB J. 22 (2008) 1135–1143.
[37] R. Zheng, K. Thompson, E. Obeng-Gyimah, D. Alessi, J. Chen, H. Cheng, T.V. McDonald, Analysis of the interactions between the C-terminal cytoplasmic domains of KCNQ1 and KCNE1 channel subunits, Biochem. J. 428 (2010) 75–84.
[38] J.D. Johnson, L.A. Wittenauer, A fluorescent calmodulin that reports the binding of hydrophobic inhibitory ligands, Biochem. J. 211 (1983) 473–479.
[39] M.V. Soldovieri, F. Miceli, G. Bellini, G. Coppola, A. Pascotto, M. Taglialatela, Correlating the clinical and genetic features of Benign Familial Neonatal Seizures (BFNS) with the functional consequences of underlying mutations, Channels (Austin) 1 (2007) 228–233.
[40] K. Dedek, B. Kunath, C. Kananura, U. Reuner, T.J. Jentsch, O.K. Steinlein, Myokymia and neonatal epilepsy caused by a mutation in the voltage sensor of the KCNQ2 K^+ channel, Proc. Natl. Acad. Sci. U. S. A. 98 (2001) 12272–12277.
[41] P. Castaldo, E. Miraglia del Giudice, G. Coppola, A. Pascotto, L. Annunziato, M. Taglialatela, Benign Familial Neonatal Convulsions caused by altered gating of KCNQ2/KCNQ3 potassium channels, J. Neurosci. 22 (2002) RC199.
[42] M.V. Soldovieri, P. Castaldo, L. Iodice, F. Miceli, V. Barrese, G. Bellini, E. Miraglia del Giudice, A. Pascotto, S. Bonatti, L. Annunziato, M. Taglialatela, Decreased subunit stability as a novel mechanism for potassium current impairment by a KCNQ2 C-terminus mutation causing Benign Familial Neonatal Convulsions, J. Biol. Chem. 281 (2006) 418–428.
[43] H.J. Chung, Y.N. Jan, L.Y. Jan, Polarized axonal surface expression of neuronal KCNQ channels is mediated by multiple signals in the KCNQ2 and KCNQ3 C-terminal domains, Proc. Natl. Acad. Sci. U. S. A. 103 (2006) 8870–8875.
[44] J.P. Cavaretta, K.R. Sherer, K.Y. Lee, E.H. Kim, R.S. Issema, H.J. Chung, Polarized axonal surface expression of neuronal KCNQ potassium channels is regulated by calmodulin interaction with KCNQ2 subunit, PLoS One 9 (2014) e103655.
[45] A. Kosenko, N. Hoshi, A change in configuration of the calmodulin-KCNQ channel complex underlies Ca^{2+}-dependent modulation of KCNQ channel activity, PLoS One 8 (2013) e82290.
[46] A. Villarroel, M. Taglialatela, G. Bernardo-Seisdedos, A. Alaimo, J. Agirre, A. Alberdi, C. Gomis-Perez, M.V. Soldovieri, P. Ambrosino, C. Malo, P. Areso, The ever changing moods of calmodulin: how structural plasticity entails transductional adaptability, J. Mol. Biol. 426 (2014) 2717–2735.
[47] W. Liu, J.J. Devaux, Calmodulin orchestrates the heteromeric assembly and the trafficking of KCNQ2/3 (Kv7.2/3) channels in neurons, Mol. Cell. Neurosci. 58 (2014) 40–52.
[48] Q. Xu, A. Chang, A. Tolia, D.L. Minor Jr., Structure of a Ca(2+)/CaM:Kv7.4 (KCNQ4) B-helix complex provides insight into M current modulation, J. Mol. Biol. 425 (2013) 378–394.
[49] K. Mruk, S.M. Shandilya, R.O. Blaustein, C.A. Schiffer, W.R. Kobertz, Structural insights into neuronal K^+ channel-calmodulin complexes, Proc. Natl. Acad. Sci. U. S. A. 109 (2012) 13579–13583.
[50] N. Gamper, Y. Li, M.S. Shapiro, Structural requirements for differential sensitivity of KCNQ K^+ channels to modulation by Ca^{2+}/calmodulin, Mol. Biol. Cell 16 (2005) 3538–3551.
[51] T. Xu, L. Nie, Y. Zhang, J. Mo, W. Feng, D. Wei, E. Petrov, L.E. Calisto, B. Kachar, K.W. Beisel, A.E. Vazquez, E.N. Yamoah, Roles of alternative splicing in the functional properties of inner ear-specific KCNQ4 Channels, J. Biol. Chem. 282 (2007) 23899–23909.
[52] M.C. Richards, S.E. Heron, H.E. Spendlove, I.E. Scheffer, B. Grinton, S.F. Berkovic, J.C. Mulley, A. Davy, Novel mutations in the KCNQ2 gene link epilepsy to a dysfunction of the KCNQ2-calmodulin interaction, J. Med. Genet. 41 (2004) e35.
[53] R. Borgatti, C. Zucca, A. Cavallini, M. Ferrario, C. Panzeri, P. Castaldo, M.V. Soldovieri, C. Baschirotto, N. Bresolin, B. Dalla Bernardina, M. Taglialatela, M.T. Bassi, A novel mutation in KCNQ2 associated with BFNC, drug resistant epilepsy, and mental retardation, Neurology 63 (2004) 57–65.
[54] D. Sachyani, M. Dvir, R. Strulovich, G. Tria, W. Tobelaim, A. Peretz, O. Pongs, D. Svergun, B. Attali, J.A. Hirsch, Structural basis of a Kv7.1 potassium channel gating module: studies of the intracellular C-Terminal domain in complex with calmodulin, Structure 22 (2014) 1582–1594.
[55] A. Kosenko, S. Kang, I.M. Smith, D.L. Greene, L.K. Langeberg, J.D. Scott, N. Hoshi, Coordinated signal integration at the M-type potassium channel upon muscarinic stimulation, EMBO J. 31 (2012) 3147–3156.